Archives of Biochemistry and Biophysics 745 (2023) 109703

Contents lists available at ScienceDirect

Archives of Biochemistry and Biophysics

journal homepage: www.elsevier.com/locate/yabbi

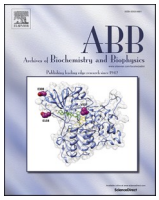

Characterization of the folding and binding properties of the PTB domain of FRS2 with phosphorylated and unphosphorylated ligands

Valeria Pennacchietti, Livia Pagano, Francesca Malagrinò [1], Awa Diop, Mariana Di Felice, Sara Di Matteo, Lucia Marcocci, Paola Pietrangeli, Angelo Toto [*], Stefano Gianni [**]

Dipartimento di Scienze Biochimiche "A. Rossi Fanelli", Sapienza Università di Roma, Laboratory affiliated to Istituto Pasteur Italia - Fondazione Cenci Bolognetti, P.le Aldo Moro 5, 00185, Rome, Italy

A R T I C L E I N F O

Handling Editor: Jose L. Neira

Keywords:
Protein-protein interactions
Stopped-flow
Site-directed mutagenesis
TrkB
FGFR1

A B S T R A C T

PTB (PhosphoTyrosine Binding) domains are protein domains that exert their function by binding phosphotyrosine residues on other proteins. They are commonly found in a variety of signaling proteins and are important for mediating protein-protein interactions in numerous cellular processes. PTB domains can also exhibit binding to unphosphorylated ligands, suggesting that they have additional binding specificities beyond phosphotyrosine recognition. Structural studies have reported that the PTB domain from FRS2 possesses this peculiar feature, allowing it to interact with both phosphorylated and unphosphorylated ligands, such as TrkB and FGFR1, through different topologies and orientations. In an effort to elucidate the dynamic and functional properties of these protein-protein interactions, we provide a complete characterization of the folding mechanism of the PTB domain of FRS2 and the binding process to peptides mimicking specific regions of TrkB and FGFR1. By analyzing the equilibrium and kinetics of PTB folding, we propose a mechanism implying the presence of an intermediate along the folding pathway. Kinetic binding experiments performed at different ionic strengths highlighted the electrostatic nature of the interaction with both peptides. The specific role of single amino acids in early and late events of binding was pinpointed by site-directed mutagenesis. These results are discussed in light of previous experimental works on these protein systems.

1. Introduction

Adaptor proteins are a class of proteins that play a pivotal role in the context of the regulation of cellular homeostasis, by acting as "scaffold" points for several signaling molecules, allowing them to form supramolecular complexes and become functional. These proteins, generally, lack catalytic activity and are composed of protein-protein interaction modules (such as SH2, SH3, PTB, and PDZ domains) by which they mediate the reversible binding with several physiological partners, for example activated RTKs [1]. Moreover, a frequent feature of scaffold proteins is the presence of large disordered regions that usually undergo post-translational modifications (such as phosphorylation), providing numerous binding sites for intracellular ligands, playing a critical role in their function, linking together different signaling pathways and coordinating complex cellular processes.

FRS2 (fibroblast growth factor receptor substrate 2) is a protein family that plays a crucial role in signaling pathways by being phosphorylated by the Fibroblast Growth Factor (FGF) and Nerve Growth Factor (NGF) receptor families [2] as well as by other RTKs involved in neuronal signaling [2–5]. Two members of FRS2 family are known, namely FRS2α and FRS2β, that share a common structural organization. FRS2α and FRS2β are characterized by the presence of a N-terminal N-myristoylation signal that anchors the protein to the plasma membrane, a Phosphotyrosine-Binding (PTB) domain, followed by a C-terminal long disordered tail with multiple tyrosine phosphorylation sites recognized by the SH2 domains of Grb2 and Shp2. Thus, FRS2 acts as a scaffold protein that organizes and facilitates the transmission of signals from FGF and NGF to downstream signaling pathways [6].

The PTB domain of FRS2 is a globular protein-protein interaction module of 115 residues structurally arranged as one α-helix flanked by two β-sheets. Its primary functional role is to recognize and bind ligands that present a phosphorylated NPXpY consensus sequences (where X is

* Corresponding author.
** Corresponding author.
E-mail addresses: angelo.toto@uniroma1.it (A. Toto), stefano.gianni@uniroma1.it (S. Gianni).
[1] Present address: Dipartimento di Farmacia, Università degli Studi di Napoli Federico II, Via Domenico Montesano 49, 80131, Naples, Italy.

https://doi.org/10.1016/j.abb.2023.109703
Received 1 June 2023; Received in revised form 25 July 2023; Accepted 26 July 2023
Available online 3 August 2023
0003-9861/© 2023 Published by Elsevier Inc.

any amino acid and pY is phosphorylated tyrosine) [7,8], although structural analysis revealed its capability to bind also unphosphorylated partners through a different topology and orientation [9,10] (Fig. 1). TrkB and FGFR1 are two typical interactors of the PTB domain of FRS2 in the intracellular environment [11,12]. TrkB is a tyrosine kinase receptor protein, with a key role in the development of the nervous system, being involved in molecular pathways that determine cell survival and neural differentiation [13,14]. Dysregulation of TrkB has been associated with various neurological diseases and behavioral disorders, as well as diverse type of cancers [15,16]. It is recognized by the PTB domain of FRS2 through the binding of a typical NPXpY sequence at the level of Y512 residue. FGFR1 is a member of the FGF receptor protein family. It is a tyrosine-protein kinase with a crucial role in the regulation of several molecular pathways which lead to embryonic development, cell proliferation, differentiation and migration, and to many genetic diseases when disrupted [17–19]. The PTB domain of FRS2 binds FGFR1 at the level of its juxtamembrane domain [9] and it is not dependent on tyrosine phosphorylation.

The function of the PTB domain of FRS2 is crucial in transducing signals from both TrkB and FGFR1 to ensure a correct cell homeostasis. However, there is a lack of information about the mechanism by which it folds in its native state to exert its functions and the determinants of its thermodynamic stability have been not established. Moreover, although structure and thermodynamics of the complex formation have been determined [8,12,20], mechanistic details of the interaction with its phosphorylated and unphosphorylated partners are still not fully understood. In this paper, we tackle these issues by providing a complete characterization of the folding and binding properties of PTB domain of FRS2 through stopped-flow kinetic experiments, conducted in a wide range of experimental conditions. Our results show that the PTB domain folds through a complex three-state mechanism implying the presence of an intermediate along the reaction. Moreover, folding experiments conducted in absence or presence of a reducing agent highlight that the disruption of a disulfide bridge affects the stability of the domain, without preventing its ability to fold in its native functional state. Kinetic binding experiments show that the PTB domain binding with the phosphorylated TrkB ligand occurs through faster kinetics compared to the unphosphorylated FGFR1. Moreover, our data put in evidence different binding mechanisms occurring through the formation of electrostatic interactions that were further analyzed by site-directed mutagenesis. Our results are discussed under the light of previous experimental works on these protein systems.

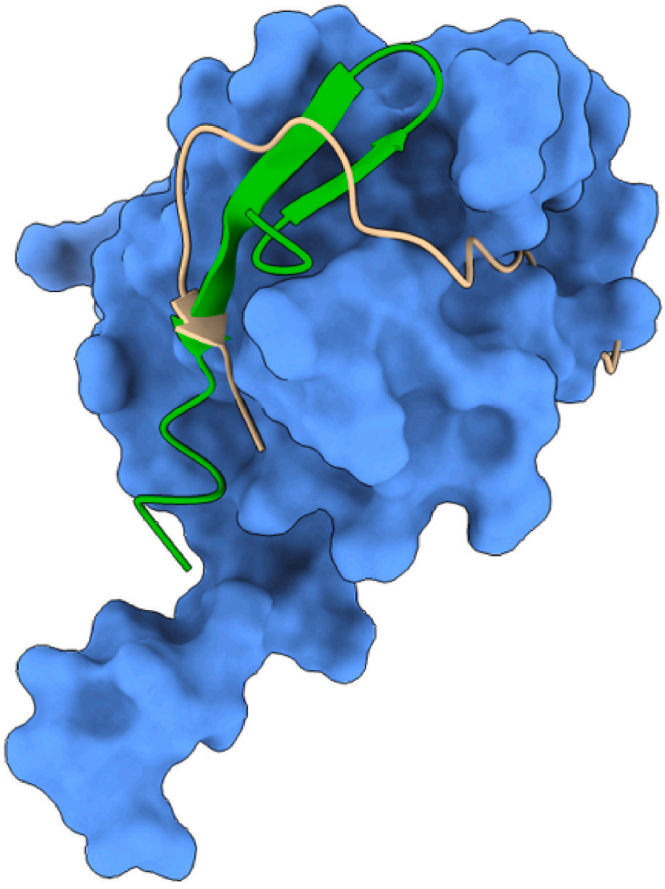

Fig. 1. Three-dimensional structure of the PTB domain of FRS2 (in blue) in complex with TrkB (in green – PDB: 2MFQ) and FGFR1 (in orange – PDB: 1XR0). The image has been obtained by using UCSF Chimera software.

2. Materials and methods

2.1. Protein expression and purification

Genes encoding for PTB, pwtPTB, and all the binding mutants were subcloned into a pET28b + vector. The pwtPTB variant, corresponding to the C91S mutation, and the PTB D27A, D28A, R63A, R64A, D68A, and R78A variants were obtained by site-directed mutagenesis QuikChange Lightning Mutagenesis Kit following manufacturer instructions. Primers oligos were purchased from Eurofins Genomics and all sequences were confirmed by DNA sequencing.

Plasmids encoding for pwtPTB and its site-directed mutants were used to transform *Escherichia coli* BL21 (DE3) competent cells. Bacterial cells were grown in LB medium containing 30 μg/mL of kanamycin at 37 °C until OD_{600} = 0.7−0.8, and protein expression was then induced with 0.5 mM IPTG. After induction, cells were grown at 25 °C overnight and then collected by centrifugation. To purify the His-tagged protein, the pellet was resuspended in buffer made of 50 mM Tris-HCl, 300 mM NaCl and 10 mM Imidazole, pH 7.5, with the addition of antiprotease tablet (Complete EDTA-free, Roche), then sonicated and centrifuged. The pellet was then resuspended with buffer containing 50 mM Tris-HCl pH 7.5 with 5 M Urea, and centrifuged. The supernatant was then loaded in a pre-equilibrated HiTrap Chelating High-Performance column (GE Healthcare). The elution was performed with a gradient of 0.01–1 M imidazole, and the imidazole was finally removed using an HiPrep desalting column (GE Healthcare), equilibrated with the buffer 50 mM Tris-HCl pH 7.5, 0.3 M NaCl. The purity of the protein sample was confirmed by sodium dodecyl sulfate polyacrylamide gel electrophoresis.

Peptides mimicking the region 493–515 of TrkB (sequence GPDAVIIGMTKIPVIENPQpYFGI) and the region 409–430 of FGFR1 (sequence HSQMAVHKLAKSIPLRRQVTVS), with and without the dansyl N-terminal modification, were purchased from GenScript.

2.2. Equilibrium (un)folding experiments

Fluorescence equilibrium (un)folding experiments were performed on a standard spectrofluorometer (FluoroMax-4 single photon counting spectrofluorometer; Horiba). The pwtPTB was excited at 280 nm, and emission spectra were recorded between 300 and 400 nm at increasing Guanidinium chloride (GdnHCl) concentrations. Experiments were performed with the protein at constant concentration of 2 μM, in 50 mM Hepes 7.0, 0.25 M Na_2SO_4, at 25 °C, using a quartz cuvette with a path length of 1 cm.

2.3. Kinetic (un)Folding experiments

Kinetic (un)folding experiments were performed on an Applied Photophysics Pi-star 180 stopped-flow apparatus, monitoring the change of fluorescence emission, exciting the sample at 280 nm, and recording the fluorescence emission using a 320 nm cutoff glass filter. The experiments were performed at 25 °C using guanidine-HCl as

denaturant agent. Buffer containing 0.25 M Na_2SO_4 used for pH dependence were: 50 mM sodium-acetate pH 5.5, 50 mM sodium-phosphate pH 6.3, 50 mM sodium-Hepes pH 7.0 and pH 7.5, 50 mM Tris-HCl pH 8.0, pH 9.0 and pH 9.5, 50 mM CHES pH 10. Kinetic (un) folding experiments in the presence of different concentrations of NaCl (0.15 M, 0.3 M, 0.5 M, 1 M) were performed in buffer Hepes 50 mM pH 7.0. For each denaturant concentration, at least five individual traces were averaged. The final protein concentration was typically 2 μM.

2.4. Kinetic binding experiments

Kinetic binding experiments were performed on an Applied Photophysics sequentialmixing DX-17MV stopped-flow apparatus (Applied Photophysics, Leatherhead, UK), set up in single mixing mode. Pseudo-first-order binding experiments were performed mixing a constant concentration (1 μM) of PTB and PTB mutants with increasing $TrkB_{493-515}$ and $FGFR1_{409-430}$, from 4 to 10 μM. Samples were excited at 280 nm, and the emission fluorescence was recorded using a 360 nm cutoff filter. For ionic strength dependence, buffers used were 50 mM sodium-HEPES pH 7.0 75 mM NaCl 50 mM sodium-HEPES pH 7.0 150 mM NaCl, 50 mM sodium-HEPES pH 7.0 300 mM NaCl, 50 mM sodium-HEPES pH 7.0 500 mM NaCl and 50 mM sodium-HEPES pH 7.0 1 M NaCl. Five traces were collected, averaged, and satisfactorily fitted to a single-exponential equation. Microscopic dissociation rate constants (k_{off}) were measured by performing displacement experiments on an Applied Photophysics sequential-mixing DX-17MV stopped-flow apparatus (Applied Photophysics), set up in single mixing mode. The observed rate constants were calculated from the average of five single traces.

3. Results

3.1. Equilibrium and kinetic (un)folding experiments

To shed light onto the folding mechanism and stability of the PTB domain of FRS2 we resorted to performing equilibrium unfolding experiments. The sequence of the PTB domain is characterized by the presence of three cysteine residues in positions 61, 80 and 91. An analysis of the three-dimensional structure highlights that the C61 and C80 are very close to each other, possibly engaging a disulfide bridge, while C91 is isolated. So, to avoid multimerization in solution we mutated C91 into serine, producing a pseudo-wild type PTB C91S (named pwtPTB from now on). Intrinsic tryptophan fluorescence of pwtPTB (W57 residue) held at constant concentration (2 μM) was followed at different concentrations of the denaturing agent GdnHCl (Guanidinium Hydrochloride). The sample was excited at 280 nm and the fluorescence emission was recorded between 300 nm and 400 nm. To measure the thermodynamic folding stability of the domain, and to test the role of disulphide bridge in the folding reaction, we conducted the experiments in buffer Hepes 50 mM, Na_2SO_4 0.25 M, pH 7.0, in the absence and in the presence of DTT at 5 mM concentration, and we plotted the measured fluorescence signal at 360 nm as function of [GdnHCl] (Fig. 2A). Data was satisfactorily fitted with a sigmoidal function [21], indicating the two-state nature of the folding reaction. From the fitting process, it is possible to calculate the midpoint of unfolding (i.e., the [GdnHCl] at which protein population is 50% unfolded and 50% native) and the $m_{D\text{-}N}$ value, that represents a measure of the cooperativity of the unfolding reaction and is directly correlated with the change in the accessible surface area upon unfolding [22]. Importantly, sharing the $m_{D\text{-}N}$ values for both datasets ($m_{D\text{-}N}$ = 2.3 ± 0.1 kcal mol^{-1} M^{-1}, compatible with a protein of 115 residues) returned an excellent fit. It is worth noticing that the presence of 5 mM DTT destabilizes the domain by ~3 kcal mol^{-1} by shifting the midpoint from

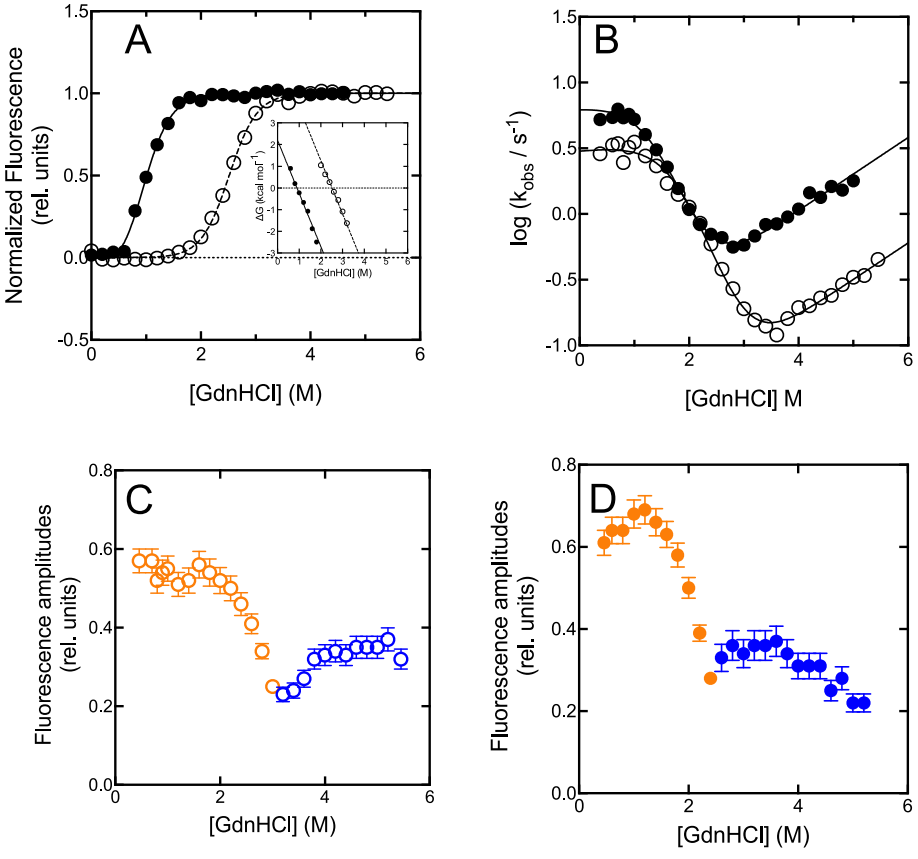

Fig. 2. A) Equilibrium unfolding experiments of the pwtPTB domain carried out at 298 K, using guanidine-HCl as denaturing agent, performed in buffer 50 mM sodium-HEPES pH 7.0, 0.25 M Na_2SO_4, in the presence (black dots) and absence (empty circles) of 5 mM DTT. Lines are the best fit to a sigmoidal equation. Inset panel: Linear free energy extrapolation. See text for details. B) Kinetic (un)folding experiments of the pwtPTB domain in the in the presence (black dots) and absence (empty circles) of 5 mM DTT. Lines are the best fit to Equation (1) (see details in the text). C) and D): Analysis of kinetic amplitudes obtained in unfolding (blue) and refolding (orange) experiments in the absence (panel C) and presence (panel D) of 5 mM DTT.

2.5 ± 0.1 M to 0.9 ± 0.1 M. The linear extrapolation of $\Delta G_{D\text{-}N}$ value (inset panel of Fig. 2A) [23] allowed to estimate $\Delta G_{D\text{-}N}$ values in the absence of denaturant (6.1 ± 0.3 kcal mol^{-1} without DTT and 2.2 ± 0.1 kcal mol^{-1} in the presence of 5 mM DTT) and $m_{D\text{-}N}$ values (2.4 ± 0.1 kcal mol^{-1} M^{-1}) that are in perfect agreement with the ones obtained by sigmoidal fitting ($\Delta G_{D\text{-}N}$ = 5.8 ± 0.1 kcal mol^{-1} in the absence of DTT and ($\Delta G_{D\text{-}N}$ = 2.1 ± 0.1 kcal mol^{-1} in the presence of 5 mM DTT). These results indicate that while the disulphide bridge formation influences the thermodynamic stability of the PTB domain, the change in accessible surface area upon unfolding is equal, and the protein is capable of folding to its native state regardless of its presence.

To obtain more detailed information about the folding of the PTB domain we performed stopped-flow kinetic (un)folding experiments. pwtPTB was rapidly diluted into solutions at different GdnHCl concentrations, samples were excited at 280 nm and the fluorescence time course was followed by using a 320 nm cut-off filter. All obtained traces were the result of averaging 3–5 independent experiments and were satisfactorily fitted to a single-exponential decay to calculate the observed rate constant (k_{obs}). The dependence of k_{obs} as function of [GdnHCl] (*i.e.*, chevron plots) obtained in buffer Hepes 50 mM, Na_2SO_4 0.25 M, pH 7.0, in the absence and presence of 5 mM DTT is reported in Fig. 2B. While for a two-state reaction, a typical V-shaped chevron plot is expected, with linear correlation between the logarithm of k_{obs} and denaturant concentration in refolding and unfolding arms, kinetic data reported in Fig. 2B report a clear deviation from linearity in the refolding arm of the chevron plots. This aspect is typically associated with the presence of an intermediate along the reaction pathway [24,25], suggesting that pwtPTB folds through a three-state mechanism. This scenario is corroborated by the analysis of the amplitudes of the kinetic traces obtained at different denaturant concentrations (Fig. 2C and D), which highlights a clear mismatch of the kinetic amplitudes obtained in refolding and unfolding experiments [25]. Given these premises, kinetic data were fitted with a three-state equation describing such scenario:

$$k_{obs} = \frac{k^0_{IN}\exp(-m_{IN}[GdnHCl])}{(1+K_{DI}\,exp(m_{DI}[GdnHCl])} + k^0_{NI}\exp(m_{NI}[GdnHCl]) \qquad \text{(Equation 1)}$$

To test the effect of a different salt on the folding kinetics, we conducted kinetic unfolding experiments in the presence of different concentrations of NaCl. Kinetic data obtained are reported in Fig. S1. Clearly, while in the presence of 5 mM DTT the chevron plot complies to a two-state scenario, in the absence of reducing agent a deviation from linearity is visible at low [GdnHCl]. This result confirms the three-state nature of the folding reaction pathway of the PTB domain, and that the presence of Na_2SO_4 in the buffer increases the stability of the intermediate, leading to a more pronounced downward curvature in the refolding arm of the chevron plot, allowing better characterization of the folding intermediate.

To further analyze the folding mechanism of the pwtPTB domain we conducted (un)folding kinetic experiments at different pH conditions, in the absence and presence of 5 mM DTT in solution. Obtained chevron plots are reported in Fig. 3A and B and kinetic and thermodynamic data obtained are listed in Table 1. Inspection of Fig. 3A and B highlight that while in the absence of DTT the change of pH appears to have nearly no effect on the folding kinetics of pwtPTB, disruption of the disulphide bridge caused an increase of k_u at basic pH conditions. Moreover, it is of interest to correlate the stability of the intermediate state as function of the stability of the native state in the presence and absence of DTT in the buffer solution. Clearly, while in the presence of the reducing agent there is no obvious correlation of the calculated $\Delta G_{D\text{-}I}$ over the $\Delta G_{D\text{-}N}$ value (slope 0.3 ± 0.1, R^2 = 0.25), in the absence of DTT we obtained a clear linear correlation (slope of 0.8 ± 0.1and an R^2 = 0.88). This result indicates that in the absence of DTT, the entropic restraints operated by the disulphide bridge between the C61 and C80 in the denatured state influences the formation of the intermediate in the early events of the folding reaction, such that the effect of pH on its thermodynamic stability well correlates with the one observed for the native state. However, our data confirm that the PTB domain can fold and reach its native state regardless of the oxidative state of C61 and C80 residues.

3.2. Kinetic binding experiments

As mentioned in the Introduction, one peculiar property of the PTB domain of FRS2 is its capability to bind phosphorylated and unphosphorylated ligands. In accordance with the structural data available, these two types of interactors engage binding through different pockets of the domain. To characterize the mechanism by which the PTB domain binds and recognizes phosphorylated and unphosphorylated ligands we conducted stopped-flow binding kinetic experiments with peptides mimicking specific regions of TrkB (from 493 to 515 residues) and FGFR1 (from 409 to 430 residues). Pseudo-first order binding experiments were conducted by rapidly mixing a constant concentration of PTB (held at 1 μM) with increasing concentrations of peptides, ranging from 4 μM to 10 μM. In analogy to previous experiments, binding reaction was followed by recording the quenching of tryptophan fluorescence emission upon binding, due to the presence of a dansyl group at the N-terminus of the peptides [26,27]. Experiments were conducted in buffer Hepes 50 mM pH 7.0 in the presence and absence of 5 mM DTT. Traces obtained resulted from averaging 3–5 independent traces and were satisfactorily fitted with a single exponential equation that allowed to calculate the observed rate constant (k_{obs}). The dependence of the k_{obs} as a function of peptide concentrations for TrkB and FGFR1 is reported in Fig. 4. Data was fitted with a linear equation

$$k_{obs} = k_{on}[peptide] + k_{off} \qquad \text{(Equation 2)}$$

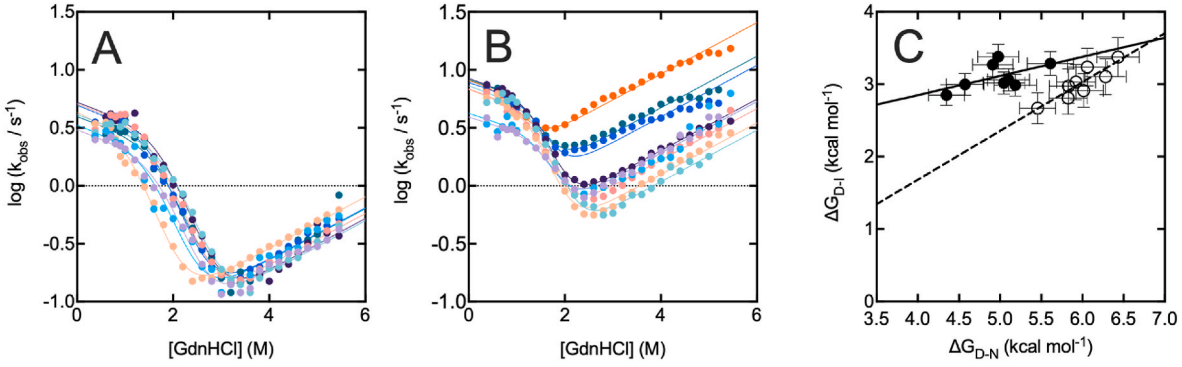

Fig. 3. Panels A and B: Kinetic (un)folding experiments of the Crkl SH2 domain at different pH conditions and 298 K. The logarithm of the observed rate constants measured with the stopped-flow apparatus is plotted versus the concentration of guanidine-HCl, in the presence (A) and absence (B) of 5 mM DTT. The lines are the best fit to a three-state model as formalized in Equation (1); Panel C: Linear correlations of the stability of the intermediate state as function of the stability of the native state in the presence (black dots) and absence (empty circles) of DTT.

Table 1
Kinetic folding parameters obtained obtained at different pH conditions, in the absence and presence of 5 mM DTT in the buffer. Errors reported are fitting errors.

	NO DTT			5 mM DTT		
	$k_{I\text{-}N}$ (s^{-1})	$k_{N\text{-}I}$ (s^{-1})	$K_{D\text{-}I}$ (s^{-1})	$k_{I\text{-}N}$ (s^{-1})	$k_{N\text{-}I}$ (s^{-1})	$K_{D\text{-}I}$
pH **5.5**	3.0 ± 0.2	0.024 ± 0.001	0.006 ± 0.001	3.7 ± 0.3	0.24 ± 0.01	0.003 ± 0.002
pH **6.3**	3.3 ± 0.2	0.030 ± 0.001	0.011 ± 0.003	4.0 ± 0.4	0.25 ± 0.01	0.004 ± 0.004
pH **7.0**	4.1 ± 0.2	0.023 ± 0.001	0.003 ± 0.001	7.2 ± 0.6	0.14 ± 0.01	0.004 ± 0.003
pH **7.5**	4.4 ± 0.4	0.037 ± 0.003	0.004 ± 0.002	6.7 ± 0.6	0.16 ± 0.01	0.006 ± 0.004
pH **8.0**	5.1 ± 0.3	0.027 ± 0.001	0.007 ± 0.002	6.7 ± 0.6	0.21 ± 0.01	0.006 ± 0.004
pH **8.5**	5.2 ± 0.3	0.024 ± 0.001	0.005 ± 0.002	8.2 ± 0.7	0.26 ± 0.01	0.006 ± 0.004
pH **9.0**	5.0 ± 0.3	0.030 ± 0.002	0.009 ± 0.002	7.3 ± 0.6	0.51 ± 0.03	0.006 ± 0.004
pH **9.5**	3.9 ± 0.2	0.030 ± 0.002	0.006 ± 0.002	7.7 ± 0.7	0.61 ± 0.03	0.008 ± 0.005
pH **10.0**	*	*	*	7.1 ± 0.9	1.20 ± 0.06	0.03 ± 0.01

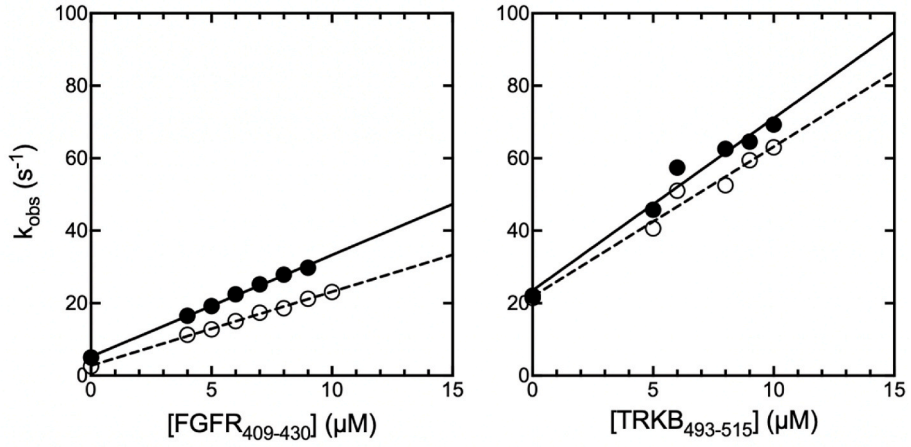

Fig. 4. Dependence of observed rate constant as a function of peptide concentrations obtained in kinetic binding experiments performed in the absence (full black circles) and presence (empty circles) of 5 mM DTT. Continuous and broken lines represent the best fit to a linear equation.

that allowed us to calculate the microscopic association rate constant (k_{on}) and extrapolate the microscopic dissociation rate constant (k_{off}) at 0 concentration of ligand. Although extrapolation of k_{off} is theoretically correct, a high error usually arises from this procedure, demanding a direct calculation of this kinetic parameter. Thus, we conducted kinetic displacement experiments, by rapidly mixing a preincubated complex of PTB (1 μM) and dansylated TrkB$_{493-515}$ or FGFR1$_{409-430}$ (4 μM) versus a high excess (50 μM) of non-dansylated variant of the peptides. Traces obtained followed a single exponential decay, and the k_{off} calculated is reported in Fig. 4 as the points at 0 μM ligand concentration. The equilibrium dissociation rate constants ($K_D = k_{off}/k_{on}$) of the PTB domain for TrkB$_{493-515}$ were 1.3 ± 0.1 μM (5 mM DTT) and 1.8 ± 0.2 μM (no DTT) and for FGFR1$_{409-430}$ were 5.9 ± 0.5 μM (5 mM DTT) and 7.0 ± 0.5 (no DTT) μM, indicating that the oxidative state of cysteine residues has a negligible effect on the binding affinity of pwtPTB.

To characterize in further detail the binding mechanism of the PTB domain with TrkB$_{493-515}$ and FGFR1$_{409-430}$ we conducted an analysis of the kinetic and thermodynamic parameters of the binding reaction changing the ionic strength of the solution. The ionic strength dependence of the binding of PTB with TrkB$_{493-515}$ and FGFR1$_{409-430}$ are reported in Fig. S2, and the obtained kinetic values are listed in Table 2. Clearly, for both peptides, an increase of the ionic strength of the solution (obtained by adding different concentrations of NaCl to a Hepes 50 mM pH 7.0 buffer) has a clear lowering effect on the k_{on} value. This result indicates that the formation of salt bridges drives the early recognition event of both peptides and resembles what is typically observed for electrostatically driven binding reactions [28,29]. On the other hand, a comparison of the effect of the ionic strength on the k_{off} put in evidence a different mechanism of the stabilization of the complex. In fact, while the k_{off} value of the binding reaction with FGFR1$_{409-430}$ cleary

Table 2
Kinetic parameters of the binding reaction between the PTB domain and FGFR1$_{409-430}$ and TrkB$_{493-515}$ at different concentrations of NaCl added to the experimental buffer. Errors reported are fitting errors and/or propagated errors.

[NaCl] (mM)	FGFR1$_{409-430}$			TrkB$_{493-515}$		
	k_{on} (μM^{-1} s^{-1})	k_{off} (s^{-1})	K_D (μM)	k_{on} (μM^{-1} s^{-1})	k_{off} (s^{-1})	K_D (μM)
150	2.3 ± 0.1	3.9 ± 0.5	1.7 ± 0.1	10.9 ± 0.3	17.1 ± 0.5	1.6 ± 0.1
300	1.59 ± 0.04	5.3 ± 0.1	3.3 ± 0.1	8.2 ± 0.3	14.6 ± 0.4	1.8 ± 0.1
500	1.18 ± 0.02	5.8 ± 0.6	4.9 ± 0.1	6.2 ± 0.3	13.2 ± 0.3	2.2 ± 0.1
1000	0.78 ± 0.02	7.8 ± 0.6	9.9 ± 0.1	3.8 ± 0.1	11.9 ± 0.3	3.1 ± 0.1

increases at higher [NaCl], highlighting a role of electrostatic forces in the late events of binding, the k_{off} for TrkB$_{493-515}$ appears to be decreased by the increasing ionic strength. This aspect reflects into a clearly different dependence of affinity for the two peptides as a function of NaCl concentrations (Fig. S3). Data show that the dependence of logK_D vs log[NaCl] for FGFR1 is much more pronounced than the one obtained for TrkB. These results suggest that in the case of TrkB binding increasing NaCl concentrations shield repulsive electrostatic forces that do not take place during the binding with FGFR1. Overall our data are in agreement with available structural data [12] and highlight a scenario in which the mechanism of recognition of both phosphorylated and unphosphorylated ligands relies on electrostatic forces, while the overall binding reaction is different, with PTB interacting with its ligands through the formation of different salt bridges.

3.3. Site-directed mutagenesis

Site-directed mutagenesis was performed to monitor the formation and roles of different charged residues in forming salt bridges involved in the recognition and stabilization of the complexes between PTB and $FGFR1_{409\text{-}430}$ and $TrkB_{493\text{-}515}$. To do so, we inspected PDB entries 1XR0 and 2MFQ, and pinpointed charged residues physically located in the binding pocket of the PTB domain. Residues D27, D28, R63, R64, D68 and R78 were mutated into alanine, and were employed in kinetic binding experiments to compare their kinetic parameters with PTB at different ionic strengths. Importantly, none of the designed mutation affected the thermodynamic stability of the PTB domain (Fig. S4). All obtained k_{obs} as function of peptides concentrations are reported in Fig. S2, and the kinetic and thermodynamic parameters calculated are listed in Table S1. Notably, D28A, R64A and R78A mutants vs $TrkB_{493\text{-}515}$ report an overall increase in k_{off} value compared to PTB wt, suggesting a role of these residues in the late event of complex stabilization (Fig. 5). However, their ionic strength dependence of the binding kinetic parameters displays a similar behavior to the wt domain. The D27A show an increase in k_{off} as the ionic strength increases, in stark contrast to what is observed for the PTB. It must be also noticed that the D68A mutation causes a dramatic decrease of k_{off} compared to wt, with a consequent increase in affinity. This result would imply the presence of electrostatic repulsion between the D68 residue and TrkB, however the analysis of the structure of the complex does not report negatively charged residues in TrkB being in direct contact with D68 of the PTB domain. The binding experiments performed with $FGFR1_{409\text{-}430}$ report the D27A mutation to almost abolish ionic strength dependence of k_{on} and k_{off}. Furthermore, the R63A mutant appears to be involved in the binding with both peptides. In binding experiments with $TrkB_{493\text{-}515}$ no kinetic traces could be recorded, indicating R63 residue to possess a key role in the binding with TrkB, while it shows a different dependence of k_{off} value compared to PTB in the binding with $FGFR1_{409\text{-}430}$, suggesting a role in stabilizing the complex rather than in recognizing the ligand in the early events of binding (Fig. 5). We also report that for the D68A mutant, we could not measure reliable kinetic traces in the binding with $FGFR1_{409\text{-}430}$ due to a dramatic decrease of kinetic amplitude, indicating a direct involvement of this residue in the binding with the peptide.

4. Discussion

FRS2 is an adapter protein forming multiprotein complexes with crucial roles in the regulation of several signaling pathways [30–34], with the PTB domain being a key mediator of such protein-protein interactions. Under this light, determining the mechanism by which the PTB domain interacts with its ligands is fundamental for a deeper understanding of the molecular pathways in which it is involved. Moreover, the characterization of its folding properties can improve our knowledge of the molecular determinants of its thermodynamic stability and of its function. Data presented in this work show that the PTB domain of FRS2 folds through a three-state folding mechanism that implies the presence of a low-energy intermediate state. It is of interest to notice how the entropic contribution of the early events of folding affects the native-like thermodynamic properties of the intermediate state. In fact, the analysis of kinetic and thermodynamic parameters reported in Fig. 3 indicate that a denatured state restrained by the formation of the disulphide bridge between C61 and C80 leads to the population of an intermediate state which is affected by the change in

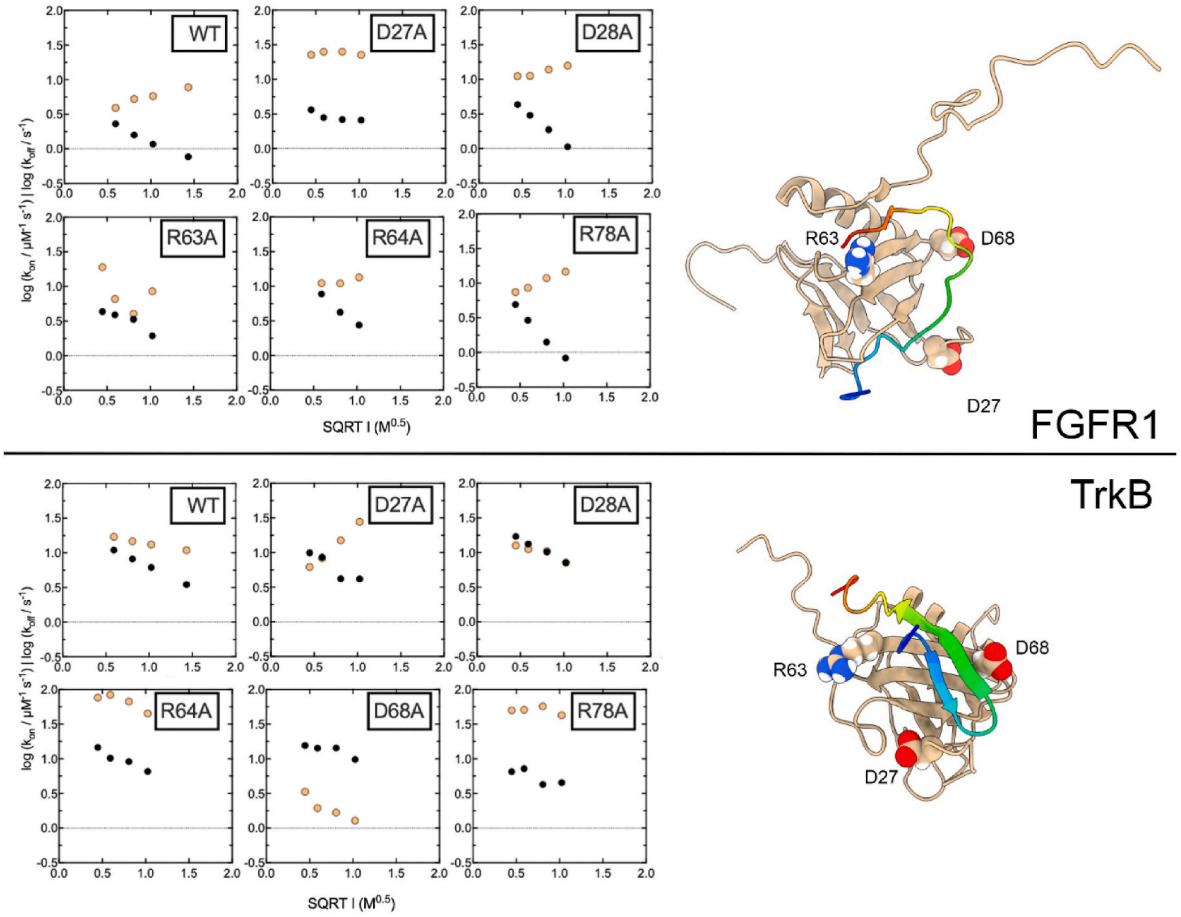

Fig. 5. Ionic strength dependences of k_{on} (black circles) and k_{off} (gold circles) parameters calculated from kinetic binding experiments for different site-directed mutants of PTB domain. Data are reported in Table S1. On the right, pinpointed positions with critical role in the binding with TrkB and FGFR1 (see text for details).

pH similarly to what occurs to the native state. These data suggest that the oxidative state of cysteine residues does not prevent proper contact formation among residues, leading the protein to collapse in its native functional state, as a funneled energy landscape would imply [35]. However, from a thermodynamic perspective, the overall folding energy landscape of the PTB domain appears to be influenced by the compactness of the denatured state, although no clear differences arise by comparing microscopic folding rate constant in the absence of denaturant. Further studies, based on extensive site-directed mutagenesis, will allow us to clarify in more details the folding pathway of the PTB domain.

As introduced previously, PTB domains can recognize ligands presenting a phosphorylated tyrosine in their sequence. In this context, their biochemical function appears to overlap with the one carried out by SH2 domains. However, the consensus sequences recognized and the mechanisms of interactions of SH2 domains and PTB domains with their ligands is largely different [36–38]. In general, the phosphorylated tyrosine of the consensus recognized by SH2 domains is of primary importance and physically accommodated in a deep, positively charged pocket in the binding cleft, while the function of PTB domains is less dependent on the presence of phosphotyrosine, that interacts with residues located on the surface of the domain. Moreover, the specificity of SH2 domains is regulated by residues located on the C-terminal side of the phosphotyrosine, while PTB domains mostly recognize N-terminal residues [36,38].

The PTB domain of FRS2 possesses the peculiar ability to interact with both phosphorylated and unphosphorylated ligands [9,30]. In an effort to characterize the mechanism of interaction with two physiological ligands, TrkB and FGFR1, we report here a detailed kinetic analysis of the binding reaction with two peptides mimicking specific portions of the interactors. Data reported in our study show that the binding with $TrkB_{493\text{-}515}$ and $FGFR1_{409\text{-}430}$ occurs with similar, low micromolar affinities. A comparison of the calculated kinetic parameters appear to be comparable to what has been previously calculated for the PTB domain of Mint2 in the binding with an unphosphorylated sequence mimicking the Amyloid Precursor Protein APP [39], an interaction that is essential for the regulation of Aβ peptide production [40,41] and that has been recently and successfully targeted with a peptide-based inhibitor [42]. The analysis of kinetic data obtained at increasing ionic strengths put in evidence a different contribution of charges in the early and late events of binding. The dependence of k_{on} and k_{off} as function of increasing ionic strengths suggest that while for TrkB charges are involved only in the early recognition events, the binding of FGFR1 is driven by electrostatic forces in both recognition and stabilization of the complex. This aspect was further investigated by site-directed mutagenesis, which allowed us to pinpoint the specific residues involved in early and late events of the binding reaction with the two different ligands. Interestingly, mutations dramatically affect the microscopic dissociation rate constant of the binding reaction with TrkB (with the exception of R63 that is directly in contact with the phosphorylated tyrosine). These data suggest that the order of events in the binding with TrkB requires first the recognition of the phosphorylated tyrosine, while other electrostatic interactions stabilize the complex formation in the late events. The binding with FGFR1 appears to be overall less affected by mutating charged residues on the binding site of PTB, with R63 and D68 residues revealing a prominent role in the binding with FGFR1. This reinforces the scenario of distinct mechanisms of binding of the PTB domain of FRS2 with phosphorylated and unphosphorylated ligands, driven by the formation of different specific salt bridges in the complex formation. Importantly, our kinetic data appear to be in good agreement with structural evidence available in literature [8,12]. Future studies based on extensive site-directed mutagenesis will allow us to further characterize these key interactions for cell physiology, to clarify possible intramolecular energetic network regulating the function of PTB domain of FRS2, and to design inhibitor molecules and/or peptides able to modulate its protein-protein interactions.

Funding sources

This work was partly supported by grants from European Union's Horizon 2020 Re- search and Innovation program under the Marie Skłodowska-Curie Grant Agreement UBIMOTIF No 860517 (to S.G.), Sapienza University of Rome (RP11715 C34AEAC9B RM1181641C2C24B9, RM11916B414C897E, RG12017297FA7223 to S. G., RM12218148DA1933 to A.T.), by an ACIP grant (ACIP 485–21) from Institut Pasteur Paris to S.G., the Associazione Italiana per la Ricerca sul Cancro (Individual Grant–IG 24551 to S.G.), the Regione Lazio (Progetti Gruppi di Ricerca LazioInnova A0375–2020–36,559 to S.G.), the Istituto Pasteur Italia ("Teresa Ariaudo Research Project" 2018, and "Research Program 2022 to 2023 Under 45 Call 2020" to A.T.). We acknowledge co-funding from Next Generation EU, in the context of the National Recovery and Resilience Plan, Investment PE8–Project Age-It: "Ageing Well in an Ageing Society". This resource was co-financed by the Next Generation EU [DM 1557 11 October 2022]. The views and opinions expressed are only those of the authors and do not necessarily reflect those of the European Union or the European Commission. Neither the European Union nor the European Commission can be held responsible for them.

Author contributions

Valeria Pennacchietti: investigation (lead), methodology (equal), formal analysis (equal), writing–review and editing (equal); Livia Pagano: investigation (equal), writing–review and editing (equal); Francesca Malagrinò;: investigation (equal), writing–review and editing (equal); Awa Diop: investigation (equal), writing–review and editing (equal); Mariana Di Felice: investigation (equal), writing–review and editing (equal); Sara Di Matteo: investigation (equal), writing–review and editing (equal);, Lucia Marcocci: investigation (equal), writing–review and editing (equal); Paola Pietrangeli: investigation (equal), writing–review and editing (equal); Angelo Toto: conceptualization (equal), formal analysis (lead), funding acquisition (equal), methodology (equal), writing–original draft preparation (lead), writing–review and editing (equal).

Stefano Gianni: conceptualization (equal), formal analysis (equal), funding acquisition (equal), methodology (equal), writing–review and editing (lead).

Appendix A. Supplementary data

Supplementary data to this article can be found online at https://doi.org/10.1016/j.abb.2023.109703.

References

[1] T. Pawson, J.D. Scott, Signaling through scaffold, anchoring, and adaptor proteins, Science 278 (1997) 2075–2080, https://doi.org/10.1126/science.278.5346.2075.
[2] H. Kouhara, Y.R. Hadari, T. Spivak-Kroizman, J. Schilling, D. Bar-Sagi, I. Lax, J. Schlessinger, A lipid-anchored Grb2-binding protein that links FGF-receptor activation to the Ras/MAPK signaling pathway, Cell 89 (1997) 693–702, https://doi.org/10.1016/s0092-8674(00)80252-4.
[3] J.B. Easton, N.M. Moody, X. Zhu, D.S. Middlemas, Brain-derived neurotrophic factor induces phosphorylation of fibroblast growth factor receptor substrate 2, J Biol Chem 274 (1999) 11321–11327, https://doi.org/10.1074/jbc.274.16.11321.
[4] Y.R. Hadari, H. Kouhara, I. Lax, J. Schlessinger, Binding of Shp2 tyrosine phosphatase to FRS2 is essential for fibroblast growth factor-induced PC12 cell differentiation, Mol Cell Biol 18 (1998) 3966–3973, https://doi.org/10.1128/MCB.18.7.3966.
[5] C. Rizzo, D. Califano, G.L. Colucci-D'Amato, G. De Vita, A. D'Alessio, N.A. Dathan, A. Fusco, C. Monaco, G. Santelli, G. Vecchio, M. Santoro, V. de Franciscis, Ligand stimulation of a Ret chimeric receptor carrying the activating mutation responsible for the multiple endocrine neoplasia type 2B, J Biol Chem 271 (1996) 29497–29501, https://doi.org/10.1074/jbc.271.46.29497.
[6] N. Gotoh, Regulation of growth factor signaling by FRS2 family docking/scaffold adaptor proteins, Cancer Science 99 (2008) 1319–1325, https://doi.org/10.1111/j.1349-7006.2008.00840.x.

[7] S.O. Meakin, J.I. MacDonald, E.A. Gryz, C.J. Kubu, J.M. Verdi, The signaling adapter FRS-2 competes with Shc for binding to the nerve growth factor receptor TrkA. A model for discriminating proliferation and differentiation, J Biol Chem 274 (1999) 9861–9870, https://doi.org/10.1074/jbc.274.14.9861.
[8] C. Dhalluin, K.S. Yan, O. Plotnikova, K.W. Lee, L. Zeng, M. Kuti, S. Mujtaba, M. P. Goldfarb, M.M. Zhou, Structural basis of SNT PTB domain interactions with distinct neurotrophic receptors, Mol Cell 6 (2000) 921–929, https://doi.org/10.1016/s1097-2765(05)00087-0.
[9] S.H. Ong, G.R. Guy, Y.R. Hadari, S. Laks, N. Gotoh, J. Schlessinger, I. Lax, FRS2 proteins recruit intracellular signaling pathways by binding to diverse targets on fibroblast growth factor and nerve growth factor receptors, Mol Cell Biol 20 (2000) 979–989, https://doi.org/10.1128/MCB.20.3.979-989.2000.
[10] N. Gotoh, S. Laks, M. Nakashima, I. Lax, J. Schlessinger, FRS2 family docking proteins with overlapping roles in activation of MAP kinase have distinct spatial-temporal patterns of expression of their transcripts, FEBS Lett 564 (2004) 14–18, https://doi.org/10.1016/S0014-5793(04)00287-X.
[11] H.R. Burgar, H.D. Burns, J.L. Elsden, M.D. Lalioti, J.K. Heath, Association of the signaling adaptor FRS2 with fibroblast growth factor receptor 1 (Fgfr1) is mediated by alternative splicing of the juxtamembrane domain, Journal of Biological Chemistry 277 (2002) 4018–4023, https://doi.org/10.1074/jbc.M107785200.
[12] L. Zeng, M. Kuti, S. Mujtaba, M.-M. Zhou, Structural insights into FRS2α PTB domain recognition by neurotrophin receptor TrkB: solution structure FRS2α PTB in complex with TrkB, Proteins 82 (2014) 1534–1541, https://doi.org/10.1002/prot.24523.
[13] Y. Iwasaki, M. Ishikawa, N. Okada, S. Koizumi, Induction of a distinct morphology and signal transduction in TrkB/PC12 cells by nerve growth factor and brain-derived neurotrophic factor, Journal of Neurochemistry 68 (2002) 927–934, https://doi.org/10.1046/j.1471-4159.1997.68030927.x.
[14] D.R. Kaplan, K. Matsumoto, E. Lucarelli, C.J. Thiele, Induction of TrkB by retinoic acid mediates biologic responsiveness to BDNF and differentiation of human neuroblastoma cells. Eukaryotic Signal Transduction Group, Neuron 11 (1993) 321–331, https://doi.org/10.1016/0896-6273(93)90187-v.
[15] V. Gupta, Y. You, V. Gupta, A. Klistorner, S. Graham, TrkB receptor signalling: implications in neurodegenerative, psychiatric and proliferative disorders, IJMS 14 (2013) 10122–10142, https://doi.org/10.3390/ijms140510122.
[16] F. Boulle, G. Kenis, M. Cazorla, M. Hamon, H.W.M. Steinbusch, L. Lanfumey, D.L. A. Van Den Hove, TrkB inhibition as a therapeutic target for CNS-related disorders, Progress in Neurobiology 98 (2012) 197–206, https://doi.org/10.1016/j.pneurobio.2012.06.002.
[17] M. Katoh, FGFR inhibitors: effects on cancer cells, tumor microenvironment and whole-body homeostasis (Review), International Journal of Molecular Medicine 38 (2016) 3–15, https://doi.org/10.3892/ijmm.2016.2620.
[18] Y.-M. Wu, F. Su, S. Kalyana-Sundaram, N. Khazanov, B. Ateeq, X. Cao, R.J. Lonigro, P. Vats, R. Wang, S.-F. Lin, A.-J. Cheng, L.P. Kunju, J. Siddiqui, S.A. Tomlins, P. Wyngaard, S. Sadis, S. Roychowdhury, M.H. Hussain, F.Y. Feng, M.M. Zalupski, M. Talpaz, K.J. Pienta, D.R. Rhodes, D.R. Robinson, A.M. Chinnaiyan, Identification of targetable FGFR gene fusions in diverse cancers, Cancer Discovery 3 (2013) 636–647, https://doi.org/10.1158/2159-8290.CD-13-0050.
[19] A. Beenken, M. Mohammadi, The FGF family: biology, pathophysiology and therapy, Nat Rev Drug Discov 8 (2009) 235–253, https://doi.org/10.1038/nrd2792.
[20] K.S. Yan, M. Kuti, S. Yan, S. Mujtaba, A. Farooq, M.P. Goldfarb, M.-M. Zhou, FRS2 PTB domain conformation regulates interactions with divergent neurotrophic receptors, J Biol Chem 277 (2002) 17088–17094, https://doi.org/10.1074/jbc.M107963200.
[21] J. Clarke, A.R. Fersht, Engineered disulfide bonds as probes of the folding pathway of barnase: increasing the stability of proteins against the rate of denaturation, Biochemistry 32 (1993) 4322–4329, https://doi.org/10.1021/bi00067a022.
[22] J.K. Myers, C. Nick Pace, J. Martin Scholtz, Denaturant *m* values and heat capacity changes: relation to changes in accessible surface areas of protein unfolding, Protein Sci 4 (1995) 2138–2148, https://doi.org/10.1002/pro.5560041020.
[23] C.N. Pace, Determination and analysis of urea and guanidine hydrochloride denaturation curves, Methods Enzymol 131 (1986) 266–280, https://doi.org/10.1016/0076-6879(86)31045-0.
[24] S. Khorasanizadeh, I.D. Peters, H. Roder, Evidence for a three-state model of protein folding from kinetic analysis of ubiquitin variants with altered core residues, Nat Struct Mol Biol 3 (1996) 193–205, https://doi.org/10.1038/nsb0296-193.
[25] S. Gianni, Y. Ivarsson, P. Jemth, M. Brunori, C. Travaglini-Allocatelli, Identification and characterization of protein folding intermediates, Biophysical Chemistry 128 (2007) 105–113, https://doi.org/10.1016/j.bpc.2007.04.008.
[26] F. Malagrinò, F. Troilo, D. Bonetti, A. Toto, S. Gianni, Mapping the allosteric network within a SH3 domain, Sci Rep 9 (2019) 8279, https://doi.org/10.1038/s41598-019-44656-8.
[27] S.R. Haq, C.N. Chi, A. Bach, J. Dogan, Å. Engström, G. Hultqvist, O.A. Karlsson, P. Lundström, L.C. Montemiglio, K. Strømgaard, S. Gianni, P. Jemth, Side-chain interactions form late and cooperatively in the binding reaction between disordered peptides and PDZ domains, J. Am. Chem. Soc. 134 (2012) 599–605, https://doi.org/10.1021/ja209341w.
[28] G. Schreiber, A.R. Fersht, Rapid, electrostatically assisted association of proteins, Nat Struct Biol 3 (1996) 427–431, https://doi.org/10.1038/nsb0596-427.
[29] F.B. Sheinerman, R. Norel, B. Honig, Electrostatic aspects of protein-protein interactions, Curr Opin Struct Biol 10 (2000) 153–159, https://doi.org/10.1016/s0959-440x(00)00065-8.
[30] H. Xu, K.W. Lee, M. Goldfarb, Novel recognition motif on fibroblast growth factor receptor mediates direct association and activation of SNT adapter proteins, J Biol Chem 273 (1998) 17987–17990, https://doi.org/10.1074/jbc.273.29.17987.
[31] A. Persaud, P. Alberts, M. Hayes, S. Guettler, I. Clarke, F. Sicheri, P. Dirks, B. Ciruna, D. Rotin, Nedd4-1 binds and ubiquitylates activated FGFR1 to control its endocytosis and function, EMBO J 30 (2011) 3259–3273, https://doi.org/10.1038/emboj.2011.234.
[32] J. Degoutin, M. Vigny, J.Y. Gouzi, ALK activation induces Shc and FRS2 recruitment: signaling and phenotypic outcomes in PC12 cells differentiation, FEBS Lett 581 (2007) 727–734, https://doi.org/10.1016/j.febslet.2007.01.039.
[33] A. Tacconelli, A.R. Farina, L. Cappabianca, G. Desantis, A. Tessitore, A. Vetuschi, R. Sferra, N. Rucci, B. Argenti, I. Screpanti, A. Gulino, A.R. Mackay, TrkA alternative splicing: a regulated tumor-promoting switch in human neuroblastoma, Cancer Cell 6 (2004) 347–360, https://doi.org/10.1016/j.ccr.2004.09.011.
[34] Y. Wu, Z. Chen, A. Ullrich, EGFR and FGFR signaling through FRS2 is subject to negative feedback control by ERK1/2, Biol Chem 384 (2003) 1215–1226, https://doi.org/10.1515/BC.2003.134.
[35] M. Oliveberg, P.G. Wolynes, The experimental survey of protein-folding energy landscapes, Quart. Rev. Biophys. 38 (2005) 245–288, https://doi.org/10.1017/S0033583506004185.
[36] P. van der Geer, T. Pawson, The PTB domain: a new protein module implicated in signal transduction, Trends Biochem Sci 20 (1995) 277–280, https://doi.org/10.1016/s0968-0004(00)89043-x.
[37] D. Cowburn, Peptide recognition by PTB and PDZ domains, Curr Opin Struct Biol 7 (1997) 835–838, https://doi.org/10.1016/s0959-440x(97)80155-8.
[38] A. Diop, D. Santorelli, F. Malagrinò, C. Nardella, V. Pennacchietti, L. Pagano, L. Marcocci, P. Pietrangeli, S. Gianni, A. Toto, SH2 domains: folding, binding and therapeutical approaches, Int J Mol Sci 23 (2022), 15944, https://doi.org/10.3390/ijms232415944.
[39] T.M.T. Jensen, C.R.O. Bartling, O.A. Karlsson, E. Åberg, L.M. Haugaard-Kedström, K. Strømgaard, P. Jemth, Molecular details of a coupled binding and folding reaction between the amyloid precursor protein and a folded domain, ACS Chem Biol 16 (2021) 1191–1200, https://doi.org/10.1021/acschembio.1c00176.
[40] J.P. Borg, J. Ooi, E. Levy, B. Margolis, The phosphotyrosine interaction domains of X11 and FE65 bind to distinct sites on the YENPTY motif of amyloid precursor protein, Mol Cell Biol 16 (1996) 6229–6241, https://doi.org/10.1128/MCB.16.11.6229.
[41] G.D. King, R.G. Perez, M.L. Steinhilb, J.R. Gaut, R.S. Turner, X11alpha modulates secretory and endocytic trafficking and metabolism of amyloid precursor protein: mutational analysis of the YENPTY sequence, Neuroscience 120 (2003) 143–154, https://doi.org/10.1016/s0306-4522(03)00284-7.
[42] C.R.O. Bartling, T.M.T. Jensen, S.M. Henry, A.L. Colliander, V. Sereikaite, M. Wenzler, P. Jain, H.M. Maric, K. Harpsøe, S.W. Pedersen, L.S. Clemmensen, L. M. Haugaard-Kedström, D.E. Gloriam, A. Ho, K. Strømgaard, Targeting the APP-mint2 protein-protein interaction with a peptide-based inhibitor reduces amyloid-β formation, J Am Chem Soc 143 (2021) 891–901, https://doi.org/10.1021/jacs.0c10696.